Spin scattering and spin-polarized hybrid interface states at a metal-organic interface

T. Methfessel,[1,*] S. Steil,[2] N. Baadji,[3] N. Großmann,[2] K. Koffler,[2] S. Sanvito,[3] M. Aeschlimann,[2]
M. Cinchetti,[2] and H. J. Elmers[1]

[1]*University of Mainz, Institute of Physics, Staudinger Weg 7, D-55128 Mainz, Germany*

[2]*Department of Physics and Research Center OPTIMAS, University of Kaiserslautern, D-67663 Kaiserslautern, Germany*

[3]*School of Physics and CRANN, Trinity College, Dublin 2, Ireland*

(Received 22 November 2011; published 9 December 2011)

Spin scattering at the interface formed between metallic Fe and Cu-phthalocyanine molecules is investigated by spin-polarized scanning tunneling spectroscopy and spin-resolved photoemission. The results are interpreted using first-principles electronic structure theory. The combination of experimental and theoretical techniques allows us to shed light on the role of hybrid interface states for the spin scattering. We show that Cu-phthalocyanine acts, via hybrid interface states, as a local spin filter up to room temperature both below and above the Fermi energy, E_F. At the same time, the molecule behaves as a featureless scattering barrier in a region of about 1 eV around E_F. Similar properties are found for both single molecules and self-assembled molecular layers, so that the acquired microscopic knowledge can be transferred to operating devices.

DOI: 10.1103/PhysRevB.84.224403 PACS number(s): 72.25.Mk, 68.37.Ef, 79.60.Fr, 81.05.Fb

Organic semiconductors (OSCs) are a class of materials dominated by π-conjugated molecules. The study of their spin properties has recently received considerable attention[1–4] because of the prospect of developing a new generation of organic spin devices. The crucial property that sets organic semiconductors apart from inorganic semiconductors is that the two most serious sources of spin relaxation, namely the spin orbit and hyperfine interactions, are predicted to be extremely small.[5] Accordingly, numerous studies have been dedicated to unveil the dominating spin-relaxation mechanisms in OSCs.[6–8]

Another unique property of OSCs is that they can form hybrid organic-inorganic interfaces displaying extremely high spin-injection efficiency.[9,10] By combining the extreme flexibility and tunability of OSCs, one may expect that hybrid interfaces will constitute a fundamental building block for advanced spintronic devices, where the spin injection will be controlled by fine-tuning the interface physical and chemical properties.[11,12] A distinctive feature of hybrid metal-organic interfaces is the presence of spin-polarized (SP) hybrid interface states (HISs).[13] These originate at a ferromagnetic metal-organic interface and affect the spin-injection efficiency across the interface itself.[10] Hence, SP-HISs are the key for understanding and thus manipulating both the sign and the magnitude of the magnetoresistance in organic spin valves.[14]

In general, the characterization of hybrid magnetic organic-inorganic interfaces is a rather complicated task. So far, two significantly different approaches have been employed. The first consists in using spin-polarized scanning tunneling microscopy and spectroscopy (SP-STM and SP-STS, respectively),[3,15] while the second utilizes spectroscopical techniques.[13] Crucially, the scanning tunneling experiments are often performed at low temperatures to explore single molecules on surfaces, while spectroscopical techniques can be easily performed at variable temperatures on molecular layers of different thicknesses. Exploiting the complementarity of both approaches is the main focus of this work, where we apply SP-STS and spin-polarized ultraviolet photoemission spectroscopy (SP-UPS) for investigating the interface formed by deposition of Cu-phthalocyanines on Fe (Fe-CuPc interface).

Such combination of experimental techniques, both corroborated by state-of-art density functional theory (DFT) calculations, gives us direct access to the interface spin-dependent electronic properties in the energy region of a few electron volts around E_F. In particular, SP-STS provides lateral resolved information at very low temperature (5 K), while SP-UPS allows us to perform thickness-dependent measurements at room temperature. Combining all the available information, we can distinguish between two energetic regions in the spin-dependent electronic structure of the interface: (i) in an energy interval of about 1 eV around E_F. the interface acts as a scattering barrier with an energy-independent spin-flip probability; and (ii) away from E_F, both in the occupied as well as in the unoccupied part of the band structure, hybrid metal-organic states form at the very interface only, as demonstrated by the thickness-dependent studies. Such HISs show spin polarization that survives up to room temperature and consequently act as local spin filters. Our findings demonstrate that the previously discussed spin filtering at E_F[3,15] does not constitute a general property of Pc molecules on a ferromagnetic substrate but strongly depends on the specific interface.

I. EXPERIMENTAL METHODS

The SP-STM and SP-STS experiments were performed in an ultrahigh vacuum triple-chamber setup (UHV, $p < 2 \times 10^{-10}$ mbar) equipped with an molecular beam epitaxy system for the deposition of metals, a low-temperature scanning tunneling microscope (Omicron LT-STM), and a chamber with a Knudson cell for evaporation of CuPc. A Mo(110) single crystal serves as substrate. The surface of the single crystal was cleaned by cycles of annealing in an oxygen atmosphere at 1200 K and subsequent flashing at 2000 K. 1.5 monolayer (ML) of Fe (99.99% purity) were deposited from a BeO crucible with a rate of 0.1 ML/min at a substrate temperature of 300 K. Subsequently, the sample was annealed at 600 K. This leads to a completely closed first Fe ML and double-layer (DL) islands. At 5 K, the ML and DL Fe/Mo(110) have an easy axis along [110], perpendicular to the surface.[16]

CuPc was deposited at 300 K at an ambient pressure of $p = 2 \times 10^{-8}$ mbar. During the deposition, the evaporation rate was monitored by a quartz balance, which in turn was calibrated by STM images.

STM measurements were performed at 5 K using chemically etched tungsten tips, which were flashed at 2200 K.[17] For SP-STS measurements, the W-Tips were covered with 10-ML Au and 5-ML Co at room temperature, leading to an out-of-plane magnetization at the tip apex. Differential conductance dI/dU maps were measured by STS in the constant-current mode using a lock-in technique. We modulated the bias voltage with 6 kHz and 50 mV amplitude. All bias voltages represent sample voltages with respect to the tip.

$I(U)$ tunneling spectra are acquired on a 2×2 grid simultaneously while measuring the topography on every second pixel of the STM image and derived afterward, leading to a spatially resolved stack of differential tunneling conductivity $dI/dU(U)$ spectra. The spectra at specific positions (e.g., on the center of the molecules, on the molecular carbon rings, and on the clean Fe surface) are extracted and averaged separately afterward for parallel and antiparallel magnetic alignment. The spectra have been normalized via the tunneling transmission function $F(S,U)$.[18] The identification of parallel ($\uparrow\uparrow$) and antiparallel ($\uparrow\downarrow$) tip-sample magnetization orientation is deduced by comparison to the spectra measured on the clean Fe/Mo(110) double layer.[19]

For the SP-UPS measurements, iron films 100 ML thick were deposited on a clean Cu(001) substrate under conditions similar to those reported in Ref. 20. The iron material (GoodFellow, 99.99% purity) was evaporated by electron bombardment at a deposition rate of 1 ML/min at a pressure of less than 1×10^{-9} mbar. The samples were annealed afterward at 450 K for 5 min. At room temperature, bulk Fe has a bcc structure, but thin Fe films grown on a Cu(001) show a fcc-like structure up to 10–11 MLs with an out-of-plane magnetization. Above that critical thickness, the morphology rearranges into small and narrow domains of bcc structure with a (110) surface orientation, similar to the Fe DL prepared for the STS experiments. Note that using the same $3d$ metal (Fe) with the same surface orientation (110) is the best approximation we could achieve in our experiments. Nevertheless, we should mention that two different lattice constants occur for the two systems. In the STM measurements, the lattice constant of the DL Fe is the lattice constant of the Mo substrate ($a = 3.14$ Å). For the UPS measurement, the lattice constant should be very similar to the Fe lattice constant ($a_{\mathrm{Fe}} = 2.87$ Å), leading to a difference of about 10%. The magnetic moment, on the other hand, switches above the critical thickness from perpendicular to in-plane orientation along the [100] direction of the Cu(001) substrate.[21] To confirm this growth mode, the crystallographic structure of the deposited iron films was investigated by low energy electron diffraction, showing patterns like those reported in Ref. 21. CuPc (1 ML) was deposited on Fe/Cu(001) with the same parameters used for the SP-STM/STS experiments described above.

The SP-UPS experiments were performed at room temperature in a μ-metal UHV system with a base pressure lower than 10^{-10} mbar, connected to the deposition chamber. The sample is irradiated with the s-polarized fourth harmonic of a 100-fs Ti:Sapphire oscillator (Spectra Physics Tsunami), with a photon energy of 5.9 eV. The laser light angle of incidence is set by geometry to 45°, and the spectra are recorded in normal emission by a commercial cylindrical sector analyzer (Focus CSA 300) equipped with a spin detector based on spin-polarized low-energy electron diffraction (Focus SPLEED).

II. THEORY METHODS

DFT calculations are performed by using the localized pseudoatomic-orbital basis and pseudopotential code SIESTA.[22] A user-optimized basis set of double-ζ quality is used to describe all the valence atomic orbitals except for O-$2p$ and N-$2p$, where additional polarized orbitals are included. The core electrons for each atomic species are described by norm-conserving Troullier-Martin pseudopotentials[23] with nonlinear core correction.[24] The generalized gradient approximation with the standard Perdew-Burke-Ernzerhof (PBE) parametrization[25] is used to describe the exchange-correlation potential.

The system setup for the theoretical simulations consists of 2 MLs of Fe relaxed over a 2-ML-thick Mo(110) surface. The Mo atomic coordinates are kept fixed at their corresponding bulk positions (lattice constant $a = 3.147$ Å). Geometry optimization is obtained by positioning a single CuPc molecule at different high-symmetry positions over the Fe/Mo(110) surface (namely the central Cu atom is placed over the top, the bridge, or the hollow site) and then by relaxing the entire molecule and the first Fe layer until the forces are smaller than 0.007 eV/Å.

The simulated STM data are obtained from DFT combined with the perturbative Bardeen approach[26] for evaluating the STM current. DFT calculations are performed using the SIESTA code.[22] STM spectra are simulated with a modified version of the Tersoff-Hamann scheme[27] where the tip is taken explicitly into account. Our STM tip consists of a flat 5-ML-thick Co surface strained to Au(100). The in-plane lattice parameter is $a = 4.08$ Å and the last 3 MLs have been relaxed vertically.

III. MORPHOLOGY

Figure 1(a) shows a STM image of CuPc molecules adsorbed on the Fe/Mo(110) ML. The molecules are oriented flat on the surface, and the four carbon rings can be clearly identified. CuPc appears in two distinct geometries over the surface distinguishable by their different apparent heights of the central atom relative to the rest of the molecule. These are strictly related to two different molecule orientations with respect to the substrate shown in Fig. 1(c). In one case, the C rings are rotated by ± 35 deg away from the substrate high-symmetry axes, [100] and [1$\bar{1}$0], and the center of the molecule appears bright. In the other case, an opposite C-ring pair is aligned parallel to these axes, with the center of the molecule appearing dark [see Fig. 1(b)]. Our theoretical calculations show that for low coverage the second geometry is energetically more favorable than the first, and Cu prefers to bind at the hollow site of the Fe surface. This is in agreement with the preferential occupation of the second site observed by STM.

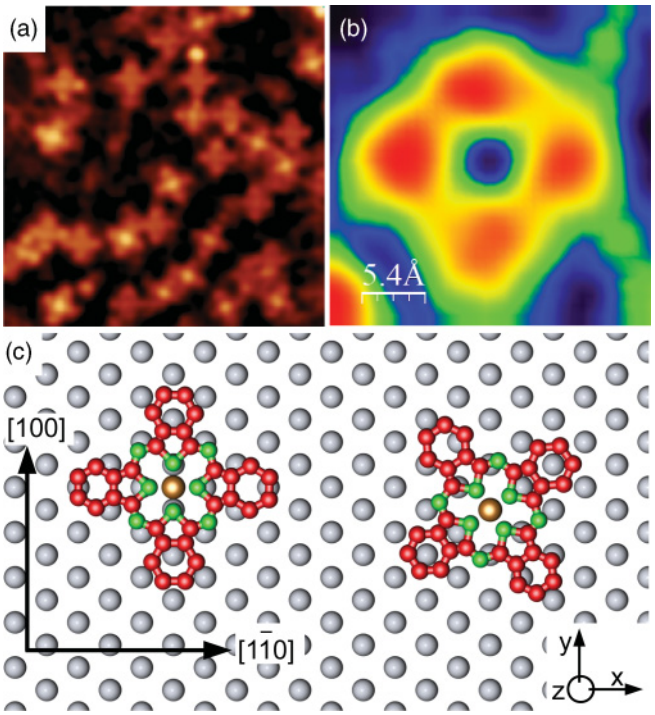

FIG. 1. (Color online) (a) STM image on the Fe ML hosting CuPc molecules [(15×15) nm^2, $U_G = 0.2$ V, and $I_T = 1.0$ nA]. The fourfold shape of the molecules can be identified as well as the two possible orientations and adsorption sites. The brightness of the central Cu atom depends on the adsorption site. (b) (2.7×2.7) nm^2 spectroscopic $I(U)$ image of a single molecule adsorbed on the Fe/Mo(110) monolayer at $E - E_F = -0.8$ V. The tip was stabilized at $U = -0.7$ V and $I = 1.0$ nA. (c) Model of the two adsorption sites for the CuPc molecules on top of the Fe/Mo(110) surface. The molecule is modeled using the UCSF CHIMERA package.[28]

At the DFT-optimized geometry shown in Fig. 2(a), the central Cu atom lies over the hollow site 1.97 Å above the Fe plane. The carbon ring extremities are respectively 3 pm below and 22 pm above the Cu, so that the molecule keeps two mirror planes (xz and yz) but loses the fourfold symmetry it possesses in vacuum. This can be seen in Fig. 2(b), where the atomic position of the carbon and nitrogen atoms of the two branches along the x and y axis are presented. When CuPc is relaxed with the Cu atom occupying the Fe top position, the Cu central atom lies above the phenyl group by about 0.4 Å and it is 2.7 Å away from Fe, which agrees with the experiment.

IV. SP-STS MEASUREMENTS

Figure 3 shows a spin-polarized dI/dU map of isolated CuPc molecules on the DL Fe/Mo(110) surface, which is extracted from a spatially resolved dI/dU-spectra stack. The Fe surface reveals a clear magnetic contrast and the C rings appear as bright rings around the dark center of the molecule.

Figures 4(a)–4(a) show the dI/dU spectra in distinct positions [on the Fe surface (a), molecule's carbon ring (b), and the molecule center (c)] acquired with STS on a 2×2 grid while simultaneously measuring the sample topography. The panels (d)–(f) show the corresponding spin asymmetry, defined as $A = [g(\uparrow\uparrow) - g(\uparrow\downarrow)]/[g(\uparrow\uparrow) + g(\uparrow\downarrow)]$. Here $g = dI/dU$

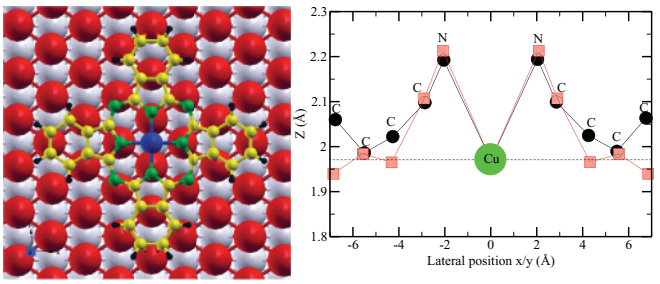

FIG. 2. (Color online) (a) Optimized geometrical structure of single CuPc deposited on two Fe MLs on top of a Mo(110) surface; (b) atomic heights relative to the free layer of Fe surface (black circles are for atoms along the x axis and red squares are for those along the y axis).

and the arrows indicate the magnetization direction of the tip and the substrate. The calculated spin asymmetry (black line) is plotted together with the experimental curves.

The spin-resolved $dI/dU(U)$ spectra of the clean Fe surface shown in Fig. 4(a) reveal two prominent peaks at -0.1 and -0.5 eV. Smaller peaks appear at $+0.1$ eV and $+0.8$ eV. Similar features have been observed previously[19] and also for the similar Fe/W(110) DL.[30] The peak near $+0.8$ eV decreases when the orientation changes from parallel to antiparallel magnetization, resulting in a double sign change of the spin asymmetry at positive energy. An opposite behavior is observed near -0.1 eV.

An attribution of the various peaks can be obtained by analogy with the similar Fe/W(110) thin film and from our DFT calculations [see Fig. 5(d)]. We assign the peak at $+0.8$ eV to the minority d_{z^2} states and that around the Fermi

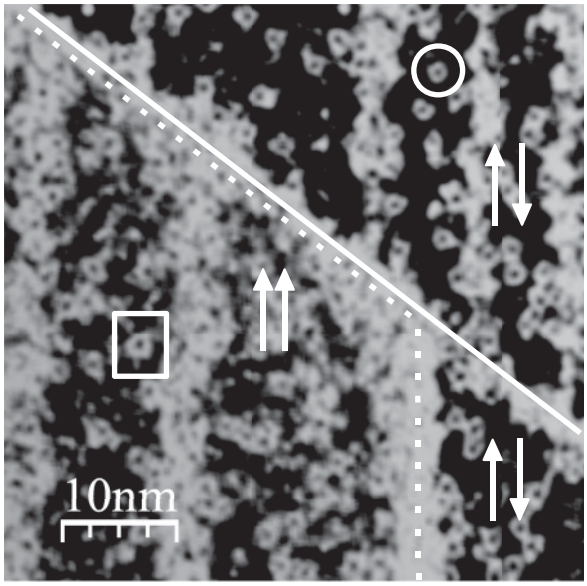

FIG. 3. Spin-polarized dI/dU map of CuPc molecules on the DL Fe/Mo(110) at $E - E_F = 143$ meV. Two molecules are marked by a circle and a square on oppositely magnetized domains, respectively, separated by the dotted line. The diagonal white line marks a step edge of the underlying Mo substrate. The broad vertical lines on the Fe surface are dislocation lines which occur in Fe/Mo(110) films due to the epitaxial misfit.[29]

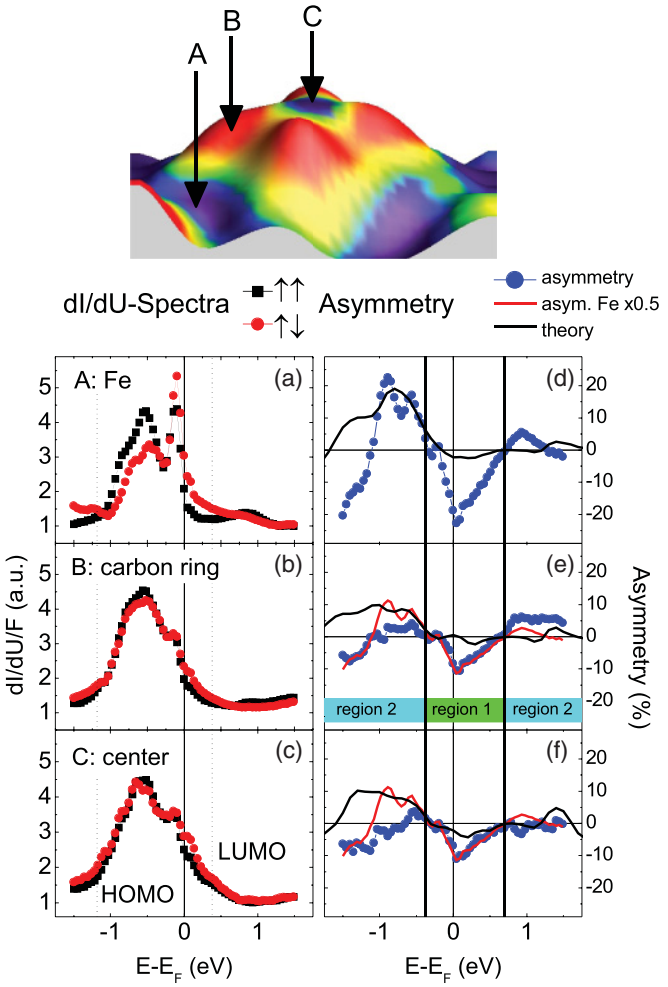

FIG. 4. (Color online) $dI/dU(U)$ spectra [(a)–(c)] and asymmetries [(d)–(f)] extracted from the indicated areas on the molecule and on the clean Fe(110) surface (circle). The STS results are compared to the calculated asymmetries (black lines). For comparison, the asymmetry of clean Fe (d) scaled by 0.5, are also shown in red lines in (e) and (f).

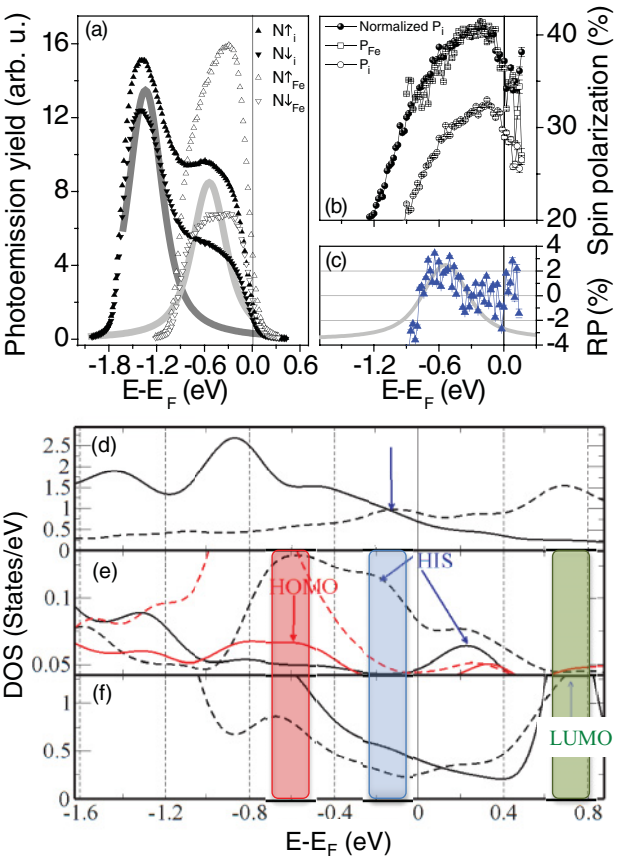

FIG. 5. (Color online) SP-UPS measurements on the Fe-CuPc interface. (a) Spectra for the majority ($N\uparrow$) and minority ($N\downarrow$) electrons on the pristine Fe substrate ($N\uparrow_{Fe}$,$N\downarrow_{Fe}$) and after deposition of 1 ML CuPc ($N\uparrow_i$,$N\downarrow_i$) and Gauss fits for the HOMO level (dark gray) and the SP-HIS (light gray). (b) Spin polarization P_{Fe} and P_i calculated from the spectra in (a) and normalized P_i. (c) Relative spin polarization (RP) of the HIS located at −0.5 eV (triangles) and Gauss fit of the HIS (gray line). Calculated DOSs for majority (solid lines) and minority (dashed lines) states, relative to the Fermi level, for Fe (d), carbon ring along the x axis (black) and the y axis (red) (e), and Cu (f).

level to a mixture of the majority d_{z^2} and the minority d_{yz}. The observed peaks below E_F at −0.5 eV and −0.8 eV are attributed to the majority d_{z^2} and d_π respectively. At around −0.1 eV, the minority density of states (DOS) becomes larger than the majority one, leading to a sign change of the spin polarization as observed in SP-STS. As far as the spin asymmetry is concerned, we first note that this depends on the spin polarization of both the sample and the tip. Although one may expect that the spin polarization of the Fe surface does not change sign over a broad energy window because of the large exchange splitting, the measured and calculated spin asymmetries [see Fig. 5(d)] display at least three sign changes in the energy range explored. These are at around −1.0, −0.3, and 0.7 eV. We assign the sign change in the spin asymmetry A at −0.3 eV to changes in the Fe spin polarization, while those at −1.0 and +0.7 eV to changes in the spin polarization of the tip.

From the STS results obtained by collecting the current at tip positions over the molecule [Figs. 4(b) and 4(c)], one can observe the almost complete suppression of the peaks at −0.1 and +0.8 eV, as compared to the clean Fe surface [Fig. 4(a)].[19,30] At the same time, a shoulder appears at +0.4 eV in the region of the unoccupied states. This is present both when the tip is over the center of the molecule and when it is placed over the C rings. Since such a shoulder is the only new feature appearing in the STS spectra, it is attributed to electronic states that originate from a weak hybridization of the lowest unoccupied molecular orbital (LUMO) of the free molecule with band states of the metallic Fe layer. The energy matches quite well with that calculated from DFT (+0.6 eV). A second weak shoulder is observed at −1.1 eV, and it is associated with states originating from weak hybridization of the highest occupied molecular orbital (HOMO). Please note that here we denote the additionally observed states HOMO and LUMO, although both states are significantly broadened due to the weak hybridization. As such, the terms HOMO and LUMO simply refer to the original molecular levels of the molecule in the gas phase participating in the hybridization process. These are identified by the DFT calculations.

Note that the HOMO-related shoulder is calculated by DFT at around −0.6 eV [see Figs. 5(e) and 5(f)]. We then end up with a STM-measured gap between the two extremal hybrid orbitals of 1.5 eV, which is in agreement with previous theoretical calculations for the HOMO-LUMO gap of the molecule in vacuum.[31] This is, however, slightly larger than that obtained in our present calculation, which returns a gap of only 1.2 eV. The differences in the calculated values can be ascribed to the different flavor of exchange and correlation functional used and to the gap renormalization expected to occur for molecules on surfaces.[32] We also note that a better match between theory and experimental results is obtained by shifting the center of the theoretical spectrum to lower energies by about 0.4 eV. Such a shift is not uncommon for molecules adsorbed on transition-metal surfaces. Notably, the calculated molecule-related spectral features appear all rather weak because of the small amplitude in the vacuum region of the local DOS of the original in-plane-oriented HOMO and LUMO orbitals (mainly $d_{x^2-y^2}$ of Cu and the π orbital of the rest of the molecule).

We now move on to discuss the STS spin asymmetries reported in Figs. 4(d)–4(f). By comparing the spin asymmetry of the clean Fe layer to that of the CuPc molecules, we can distinguish two regions, denoted as regions 1 and 2. Region 1 is in the vicinity of E_F and ranges approximately between −0.3 and +0.7 eV. Here, although the overall $dI/dU(U)$ spectrum of the molecule changes significantly from that of Fe(110) and the LUMO level appears at +0.4 eV (+0.6 eV in the calculated spectra), the spectral features of the spin asymmetry A are only slightly modified with the exception of a global reduction of A by about 50%. This is demonstrated in Figs. 4(e) and 4(f), where A for Fe(110) is re-scaled by a factor 0.5 and superimposed on that of CuPc. Such behavior can be explained by assuming that the Fe-CuPc interface acts as a featureless scattering barrier displaying an energy-independent spin-flip probability, which results from the low density of hybridized states close to the Fermi energy. This is remarkable considering that in previous experiments on Co-CoPc[3] and Fe-CoPc[15] interfaces, the spin-dependent tunneling from the ferromagnetic substrate at E_F was strongly modified by the presence of the molecule. Thus, we conclude that this is not a general behavior, but instead it strongly depends on the specific interface as well as on the Pc's central atom.

Region 2 is the one below −0.3 eV and above +0.7 eV. In this range, A presents pronounced deviations from that for the Fe surface either when the current is collected from the carbon rings or from the central Cu atom. Such a behavior will be explained below with the help of the SP-UPS results and the *ab initio* calculations.

V. SP-UPS MEASUREMENTS

Figure 5 shows the results of the SP-UPS measurements on the (100-ML) Fe/(1-ML) CuPc interface together with the calculated DOS for both Fe and the Fe/CuPc interface. Panel (a) displays the spectra for the majority ($N\uparrow$) and minority ($N\downarrow$) electrons collected for the pristine Fe substrate ($N\uparrow_{\mathrm{Fe}}$, $N\downarrow_{\mathrm{Fe}}$) and after deposition of 1-ML CuPc ($N\uparrow_i$, $N\downarrow_i$). The latter contains information about the spin-dependent electronic

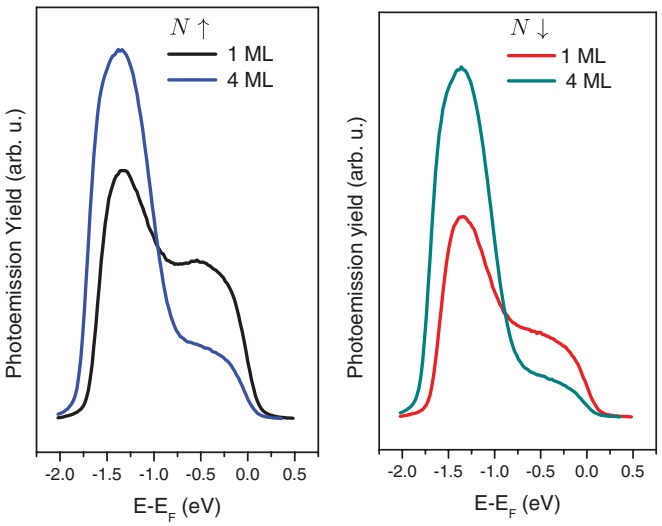

FIG. 6. (Color online) Comparison of the SP-UPS measurements on the Fe-CuPc system performed for different CuPc thicknesses (1 ML and 4 ML). The left panel shows the majority spectra ($N\uparrow$) recorded for the two different thicknesses, and the right panel shows the minority spectra ($N\downarrow$).

structure of the Fe-CuPc interface and can be thus compared to the calculations in panels (d)–(f). There are two major features in the interface spectra: a peak in both majority and minority spectra centered at −1.2 eV (Gauss fit shown with a dark grey line) and a second peak located at −0.5 eV in the majority spectrum only (Gauss fit shown with bright gray line). To first discern whether such features are interface- or bulk-(CuPc) related, we performed thickness-dependent measurements. We prepared samples with variable CuPc thickness, starting from 1 ML up to 4 MLs. Figure 6 shows the $N\uparrow$ (left panel) and $N\downarrow$ (right panel) spectra recorded for 1-ML and 4-ML CuPc. The $N\uparrow,\downarrow$ spectra contain three contributions. They are given by (i) the electrons excited in the topmost CuPc layer, (ii) the electrons originating from the Fe-CuPc interface, and (iii) the electrons excited in the Fe substrate. The electrons originating from (ii) and (iii) can be photoemitted after having reached the topmost CuPc layer, if they are excited within the electron mean free path, $\lambda \approx 1$ nm.[33] This means that by increasing the CuPc thickness, the contribution of the photoemission yield from the Fe-CuPc interface is progressively reduced. Accordingly, features of the photoemission spectra that are progressively suppressed by increasing CuPc thickness can be unequivocally attributed to interface-related features. On the other hand, features whose spectral weight increases by increasing CuPc coverage must be related to the electronic structure of bulk CuPc.

An inspection of the spectra in Fig. 6 reveals that while the spectral weight of the peak centered at −1.2 eV in the 1-ML spectra increases by increasing CuPc thickness, the peak at −0.5 eV vanishes for 4-ML coverage. This brings us to the following conclusions: the peak centered at −1.2 eV in Fig. 5(a) can be attributed to electronic states originating from weak hybridization of the HOMO with band states of the Fe, in good agreement with the position of the HOMO measured by STS (−1.1 eV). The peak centered at −0.5 eV in Fig. 5(a), on the other hand, corresponds to a HIS, which lies energetically

between the previously identified HOMO and LUMO levels and is only present at the Fe-CuPc interface.

In order to determine the spin polarization of the HIS located at −0.5 eV in the SP-UPS measurements shown in Fig. 5(a), we proceed as follows. We calculate the spin polarization of the Fe substrate (P_{Fe}) as well as that of the Fe-CuPc interface (P_i), by using the common definition $P = (N\uparrow - N\downarrow)/(N\uparrow + N\downarrow)$. The two quantities are plotted in Fig. 5(b). P can be directly compared to the calculated spin-resolved DOS, and it is connected to the STS spin asymmetry A via $A = P_{\mathrm{SP-UPS}} P_{\mathrm{tip}}$, where P_{tip} is the spin polarization of the tip. We first note that P_{Fe} and P_i have the same shape, while $|P_i| < |P_{\mathrm{Fe}}|$. Since the mean free path of the excited photoelectrons is less than 1 nm,[33] the $N\uparrow_i$,$N\downarrow_i$ spectra, and thus P_i, contain two contributions. They are given by (i) the electrons originating from the Fe-CuPc interface and (ii) the electrons excited by the laser pulse in the Fe substrate that can be photo-emitted after crossing the Fe-CuPc interface, if they are excited within the electron mean free path. If the interface possesses a band gap in a certain energy range (ΔE), than P_i will have (within ΔE) the same shape as P_{Fe}. In other words $P_i/P_{\mathrm{Fe}} = C$, where $C \leqslant 1$ is a constant.

The lower absolute value of P_{Fe} compared to that of P_i (i.e., $C < 1$) is due to spin-flip events taking place at the Fe-CuPc interface. For an easier comparison, we have rescaled P_i by 0.785, leading to the curve depicted in Fig. 5(b) (full black circles). Between −0.4 and 0 eV, the normalized P_i follows perfectly P_{Fe}, in agreement with the behavior of the asymmetry measured by SP-STS. This is also supported by the DOS calculated for the Fe free surface and for the CuPc decorated one [Figs. 5(d)–5(f)]. Since this energetic region lies within the HOMO-LUMO gap, CuPc is transparent to the polarized electrons extracted from the Fe layer below.

Below −0.4 eV, the normalized P_i lies slightly above P_{Fe}, suggesting that the HIS located around −0.5 eV is spin polarized. In order to confirm this hypothesis, we normalize the $N\uparrow_i$,$N\downarrow_i$ curves respectively to $N\uparrow_{\mathrm{Fe}}$,$N\downarrow_{\mathrm{Fe}}$ in the energy range between −0.06 and 0.14 eV, where the Fe and interface spectra have the same shape. The obtained normalization factors for the majority and minority spectra are $\gamma\uparrow = 2.34$, $\gamma\downarrow = 1.93$. We can then calculate the spin polarization by using the normalized $\tilde{N}\uparrow_i$,$\tilde{N}\downarrow_i$ spectra according to $\mathrm{RP} = (\tilde{N}\uparrow_i - \tilde{N}\downarrow_i)/(\tilde{N}\uparrow_i + \tilde{N}\downarrow_i)$. The quantity RP represents the spin polarization of the HIS relative to the spin polarization of the iron substrate. It is plotted in Fig. 5(c), together with the Gauss fit of the HIS from Fig. 5(a), clearly demonstrating that the HIS at −0.5 eV possesses a positive spin polarization.

VI. DISCUSSION AND SUMMARY

We now focus our discussion on the properties of the spin-polarized hybrid state detected both by STS and SP-UPS. This state originates from the interaction of CuPc molecular orbitals with band states of the iron. Its presence can be clearly seen also in the DOS calculations presented in Figs. 5(e) and 5(f). In Fig. 5(e), we show the DOS of two carbon atoms lying on the ring either along the x axis (black) or the y axis (red). One can immediately see that, in addition to the calculated HOMO and LUMO (respectively at −0.6 and 0.6 eV), two additional peaks are present at around ±0.2 eV. These states

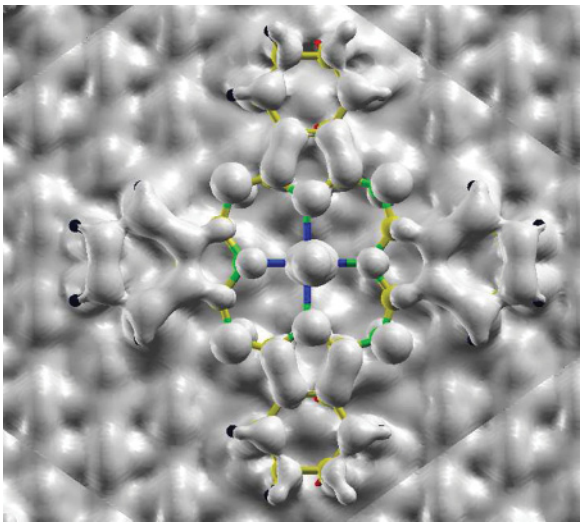

FIG. 7. (Color online) Local density of states integrated between −0.3 and −0.2 eV showing the HIS.

are positioned in the HOMO-LUMO gap of the free molecule and, as such, they are hybrids between Fe d_{yz}, Cu d_{z^2}, and an extended π-like orbital spreading over the rest of the molecule. The state at −0.2 eV is also visible in Fig. 5(f), which shows the calculated DOS for the Cu. Such an interface-induced gap state is identified as the HIS. The local DOS associated to such an HIS is shown in Fig. 7. One can immediately see that the actual state is a combination of a spread Fe d_π orbital, the d_z^2 Cu orbital, and an extended π state distributed over the rest of the CuPc molecule.

Interestingly, the spin polarization P for the two hybrid states emerging from the DOS calculations at ±0.2 eV is different when calculated either on Cu or on C. The peak below E_{F} has a positive spin polarization on Cu and negative one on the C ring, while for the one above E_{F} the situation is reversed. Such a spatially dependent spin-polarization inversion was recently reported for a similar system.[15] Note that the positive spin polarization of the HIS at −0.5 eV measured with SP-UPS agrees with the DOS calculations (Fig. 5). In fact, at the energetic position of the HIS, we predict a DOS higher on the Cu than on C. Being the theoretical P on Cu positive, the *net* spin polarization as measured by a spatially integrating detection technique like SP-UPS would be positive as well. Importantly, the SP-UPS measurements demonstrate that the spin polarization of the HIS is preserved up to room temperature.

The presence of SP-HISs at the Fe/CuPc interface finally allows us to interpret the behavior of the SP-STS spin asymmetry in region 2 of Fig. 4. In fact, every SP-HIS appearing in the DOS provides a contribution to the tunneling current measured by SP-STS. This results in a modification of the energy-dependent spin asymmetry A of the Fe surface. As such when A is calculated by using the STS currents measured with the tip positioned over the molecule, its energy profile will no longer have the same shape as when the current is collected directly over Fe. Therefore, the spin asymmetry A as a function of $(E - E_F)$ gives direct information on the spin polarization of the HISs. An inspection of A in Figs. 4(e) and 4(f) reveals the presence of a HIS at −0.5 eV with positive SP

and localized both over C and Cu. Furthermore, two additional HISs, which are out of the range detectable with SP-UPS, can be distinguished in the STS asymmetry A. The first is located at around -1 eV, and the second is at $+0.6$ eV. They both possess a positive spin polarization over the carbon rings and a negative one over the CuPc center.

Also, these two states can be identified in the calculated DOS, although their precise energy position is affected by the DFT gap problem. By keeping this in mind, the HIS located at 0.6 eV is associated with the calculated one at $+0.2$ eV, while the one below E_F in SP-UPS is associated with the calculated one at -0.2 eV. It is also worth mentioning that the spin polarization measured on the C ring is closer to that of Fe than that measured on Cu. This fact may be interpreted as the effect of a reduced HIS density at the C position compared to that of the Cu.

In summary, despite the differences in the lattice constants and in the magnetic anisotropy of the used Fe films, we find a general agreement between the SP-STS and SP-UPS data, which points to the fact that the fundamental interaction process of the CuPc molecular orbitals with the Fe band states is very similar in the two systems. In particular, by comparing SP-STS and SP-UPS measurements and DFT calculations for the Fe(110)-CuPc interface, we could distinguish two characteristic regions in the interface electronic structure: (i) close to E_F, no SP-HISs are present and the interface acts as a featureless scattering barrier with an energy-independent spin-flip probability; and (ii) away from E_F, the spin-dependent tunneling probability is dominated by SP-HISs, whose spin polarization is preserved up to room temperature. SP-HISs lead to a modification of the energy dependence of the Fe asymmetry and spin polarization. Our results indicate that the energy of the SP-HISs can be modified by the choice of the central atom in phthalocyanines. In particular, for CuPc the detected SP-HISs are energetically away from E_F. As a consequence, the energy dependence of the spin polarization of the underlying ferromagnetic layer is preserved for spin transport in CuPc near E_F.

ACKNOWLEDGMENTS

Financial support from DFG Research Grant No. AE 19/8-2 is gratefully acknowledged. N.B. and S.S. thank the Science Foundation of Ireland (Grant No. 08/ERA/I1759) and CRANN for financial support. The research leading to these results was partly funded from the European Union Seventh Framework Programme (FP7/2007 -2013) under grant agreement n° 263104.

*methfess@uni-mainz.de

[1] V. A. Dediu, L. E. Hueso, I. Bergenti, and C. Taliani, Nat. Mater. **8**, 707 (2009).
[2] N. Atodiresei, J. Brede, P. Lazic, V. Caciuc, G. Hoffmann, R. Wiesendanger, and S. Blugel, Phys. Rev. Lett. **105**, 066601 (2010).
[3] C. Iacovita, M. V. Rastei, B. W. Heinrich, T. Brumme, J. Kortus, L. Limot, and J. P. Bucher, Phys. Rev. Lett. **101**, 116602 (2008).
[4] H. Wende *et al.*, Nat. Mater. **6**, 516 (2007).
[5] S. Sanvito, J. Mater. Chem. **17**, 4455 (2007).
[6] N. J. Rolfe, M. Heeney, P. B. Wyatt, A. J. Drew, T. Kreouzis, and W. P. Gillin, Phys. Rev. B **80**, 241201 (2009).
[7] T. D. Nguyen, G. Hukic-Markosian, F. Wang, L. Wojcik, X.-G. Li, E. Ehrenfreund, and Z. V. Vardeny, Nat. Mater. **9**, 345 (2010).
[8] P. A. Bobbert, W. Wagemans, F. W. A. van Oost, B. Koopmans, and M. Wohlgenannt, Phys. Rev. Lett. **102**, 156604 (2009).
[9] S. Sanvito, Nat. Phys. **6**, 562 (2010).
[10] M. Cinchetti, S. Neuschwander, A. Fischer, A. Ruffing, S. Mathias, J.-P. Wüstenberg, and M. Aeschlimann, Phys. Rev. Lett. **104**, 217602 (2010).
[11] M. E. Ali, B. Sanyal, and P. M. Oppeneer, J. Phys. Chem. C **113**, 14381 (2009).
[12] L. Schulz *et al.*, Nat. Mater. **10**, 39 (2011).
[13] Y. Zhan, E. Holmstr om, R. Lizárraga, O. Eriksson, X. Liu, F. Li, E. Carlegrim, S. Stafstr om, and M. Fahlman, Adv. Mater. **22**, 1626 (2010).
[14] C. Barraud *et al.*, Nat. Phys. **6**, 615 (2010).
[15] J. Brede, N. Atodiresei, S. Kuck, P. Lazic, V. Caciuc, Y. Morikawa, G. Hoffmann, S. Blugel, and R. Wiesendanger, Phys. Rev. Lett. **105**, 047204 (2010).
[16] A. Kukunin, J. Prokop, and H. J. Elmers, Phys. Rev. B **76**, 134414 (2007).
[17] M. Bode, Rep. Prog. Phys. **66**, 523 (2003).
[18] V. A. Ukraintsev, Phys. Rev. B **53**, 11176 (1996).
[19] J. Prokop, A. Kukunin, and H. J. Elmers, Phys. Rev. B **73**, 014428 (2006).
[20] O. Andreyev *et al.*, Phys. Rev. B **74**, 195416 (2006).
[21] F. Scheurer, R. Allenspach, P. Xhonneux, and E. Courtens, Phys. Rev. B **48**, 9890 (1993).
[22] J. M. Soler, E. Artacho, J. D. Gale, A. Garcia, J. Junquera, P. Ordejón, and D. Sanchez-Portal, J. Phys. Condens. Matter **14**, 2745 (2002).
[23] N. Troullier and J. L. Martins, Phys. Rev. B **43**, 8861 (1991).
[24] J. Zhu, X. W. Wang, and S. G. Louie, Phys. Rev. B **45**, 8887 (1992).
[25] J. P. Perdew, K. Burke, and M. Ernzerhof, Phys. Rev. Lett. **77**, 3865 (1996).
[26] J. Bardeen, Phys. Rev. Lett. **6**, 57 (1961).
[27] N. Baadji, S. Kuck, J. Brede, G. Hoffmann, R. Wiesendanger, and S. Sanvito, Phys. Rev. B **82**, 115447 (2010).
[28] E. F. Pettersen, T. D. Goddard, C. C. Huang, G. S. Couch, D. M. Greenblatt, E. C. Meng, and T. E. Ferrin, J. Comput. Chem. **25**, 1605 (2004).
[29] S. Murphy, G. Mariotto, N. Berdunov, and I. V. Shvets, Phys. Rev. B **68**, 165419 (2003).
[30] M. Bode, A. Kubetzka, O. Pietzsch, and R. Wiesendanger, Surf. Sci. **514**, 135 (2002).
[31] M. Cinchetti, K. Heimer, J. P. Wustenberg, O. Andreyev, M. Bauer, S. Lach, C. Ziegler, Y. L. Gao, and M. Aeschlimann, Nat. Mater. **8**, 115 (2009).
[32] J. B. Neaton, M. S. Hybertsen, and S. G. Louie, Phys. Rev. Lett. **97**, 216405 (2006).
[33] S. Steil, K. Goedel, A. Ruffing, I. Sarkar, M. Cinchetti, and M. Aeschlimann, Synth. Met. **161**, 570 (2011).